Rigidity analysis of T3R1 parallel robot with uncoupled kinematics

B. C. Bouzgarrou, J.C. Fauroux, G. Gogu, Y. Heerah

Laboratoire de Recherche et Applications en Mécanique avancée (LaRAMA)
Institut Français de Mécanique Avancée (IFMA) et Université Blaise Pascal
Campus universitaire de Clermont-Ferrand/ Les Cézeaux, BP265, 63175 Aubière France
Tel : 33.4.73.28.80.00, E-mail : bouzgarr/fauroux/gogu@ifma.fr

Abstract

Complexity for common parallel robots is mainly due to kinematic coupling between joint and operational space coordinates. Designing a parallel robot with uncoupled kinematics, such a Cartesian robot, simplifies considerably robot modeling and control. In this paper we study static and dynamic rigidity of a new parallel platform in order to optimize mechanical design and control strategy. This parallel robot with four degrees of mobility and pseudo-decoupled motions is developed at LaRAMA - French Institute of Advanced Mechanics.

1 Introduction

This paper presents rigidity analysis of a new parallel mechanism with four degrees of mobility and decoupled motions. This parallel robot, called *T3R1*, is issued from a general structural synthesis approach of parallel platform mechanisms with 2, 3, 4, 5 and 6 degrees of mobility and decoupled motions. This approach and the structural solutions are extensively presented in [1]. All independent motions of these robots can be partially or entirely decoupled. In a parallel platform mechanism with entirely decoupled motions, the Jacobian matrix of the linear transformation (mapping) between the joint velocity space and the operational velocity space is a diagonal matrix. A one-to-one correspondence exists between the end-effector output velocities and the input joint velocities. Several types of *TPM* (3-leg 3-degrees of mobility translational parallel manipulators) with decoupled motions are presented by Hervé and Sparacino [2], Carricato and Parenti-Castelli [3], Kim and Tsai[4], Kong and Gosselin [5]. *T3R1* adds a supplementary rotation and implicitly a supplementary leg and supplementary joints to the structure of a spatial *3-PRRR* parallel manipulator *TPM*-type.

One of the commonly admitted advantages of parallel robots over serial robots is their improved rigidity [6]. Parallel robots with decoupled motions such as *T3R1* have a wide range of potential applications in manipulation, assembling and machining. This paper focus on the static rigidity of *T3R1* in order to evaluate its performance for real applications.

2 Kinematic structure

T3R1 is composed of a mobile platform (*5*) and a base (*0*) connected by four legs (*A, B , C* and *D*) in parallel (Figs. 1 and 2). Under the action of the total constraints of its four legs, the mobile platform can do three independent translations (x_H, y_H, z_H) and one rotation φ_a (a=x,y,z). The solutions presented in Figs. 1 and 2 allow a rotation on y axis (a=y). Each leg in Fig. 1 has three revolute joints with axes parallel to the direction of ground-connected prismatic joint. Mobile platform is connected by two revolute joints parallel to a axis (a=y). Furthermore, the three prismatic joint axes on the legs *A, B* and *C* are parallel to x_0, y_0, and z_0 axes, respectively.

The ground-connected prismatic joint axis on the leg *D* is also parallel to z_0 axis. The four ground-connected prismatic joints are actuated. The four independent joint variables are d_{10A}, d_{10B}, d_{10C} and d_{10D}. The direct kinematic model of the solution presented in Fig. 1, defined by the matrix mapping between the joint velocity space ($\dot{d}_{10A},\dot{d}_{10B},\dot{d}_{10C},\dot{d}_{10D}$) and the operational space ($\dot{x}_H,\dot{x}_H,\dot{x}_H,\dot{\varphi}_y$) is :

$$\begin{bmatrix}\dot{x}_H\\ \dot{y}_H\\ \dot{z}_H\\ \dot{\varphi}_y\end{bmatrix}=\begin{bmatrix}1&0&0&0\\0&1&0&0\\0&0&1&0\\0&0&b_{43}&b_{44}\end{bmatrix}\begin{bmatrix}\dot{d}_{10A}\\ \dot{d}_{10B}\\ \dot{d}_{10C}\\ \dot{d}_{10D}\end{bmatrix} \tag{1}$$

with

$$b_{43}=-b_{44}=\frac{-1}{r\cos\varphi_y}. \tag{2}$$

From Eq. (1) we can see that this parallel robot achieves a one-to-one correspondence between the joint velocities $\dot{d}_{10A},\dot{d}_{10B},\dot{d}_{10C}$ and the operational translation velocities $\dot{x}_H,\dot{x}_H,\dot{x}_H$ but the rotation velocity $\dot{\varphi}_y$ depends on the difference $\dot{d}_{1D1C}=\dot{d}_{10D}-\dot{d}_{10C}$

$$\dot{\varphi}_y=\frac{1}{r\cos\varphi_y}(\dot{d}_{10D}-\dot{d}_{10C})=\frac{\dot{d}_{1D1C}}{r\cos\varphi_y}. \tag{3}$$

This robot has pseudo-decoupled motions. We can consider that a one-to-one correspondence exist between $\dot{\varphi}_y$ and $\dot{d}_{1D1C}$.

To obtain decoupled motions between $\dot{d}_{10A},\dot{d}_{10B},\dot{d}_{10C},\dot{d}_{1D1C}$ and $\dot{x}_H,\dot{x}_H,\dot{x}_H,\dot{\varphi}_y$ we can use the solution presented in Fig.2. In this case, the prismatic joint axis on the leg *D* is not ground-connected. This prismatic joint connects the kinematic elements 1_C and 1_D.

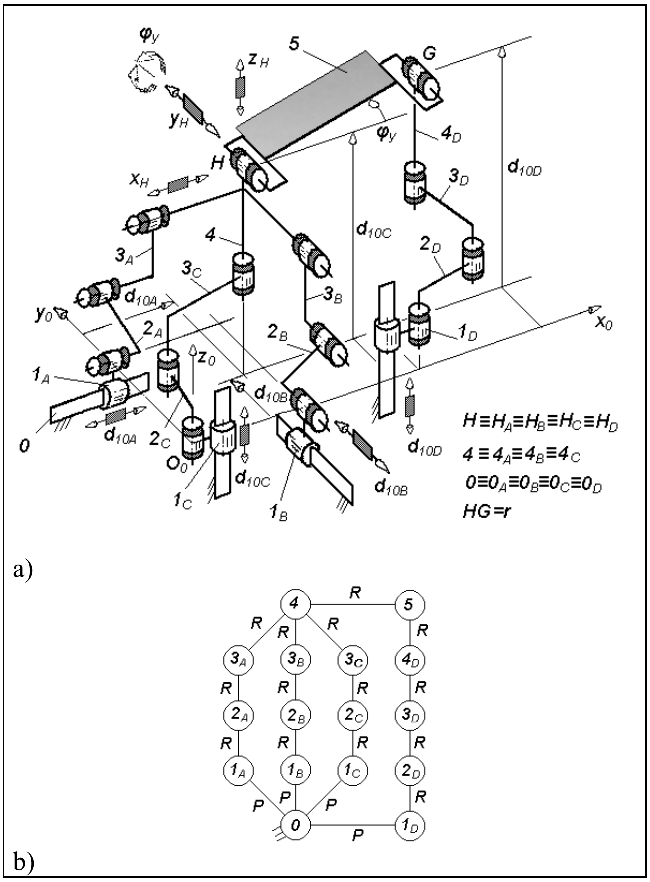

FIG 1. Parallel platform mechanism T3R1 with pseudo-decoupled motions: a) kinematic structure, b) associated graph (from Gogu, 2002 [1])

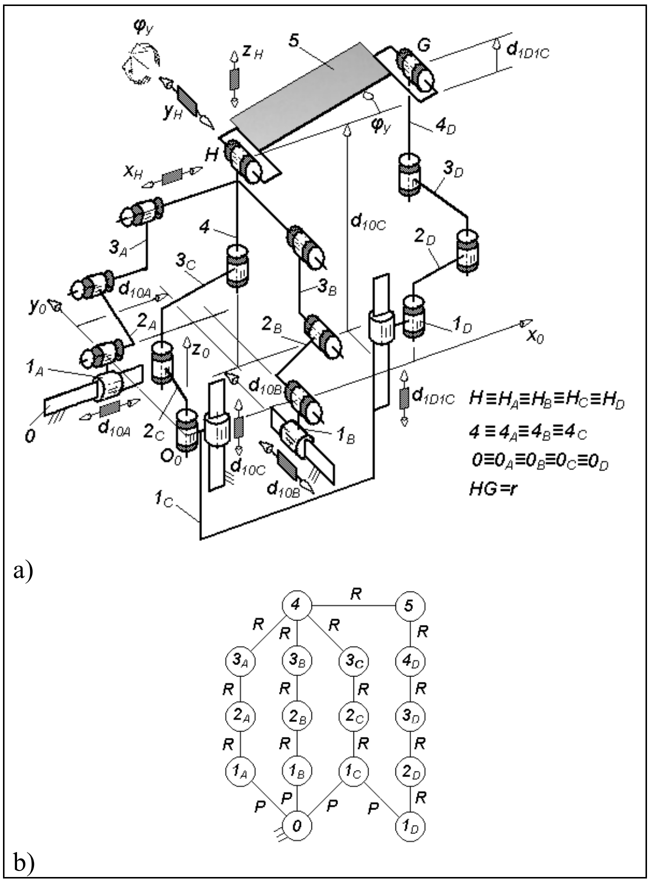

FIG 2. Parallel platform mechanism T3R1 with decoupled motions: a) kinematic structure, b) associated graph (from Gogu, 2002 [1])

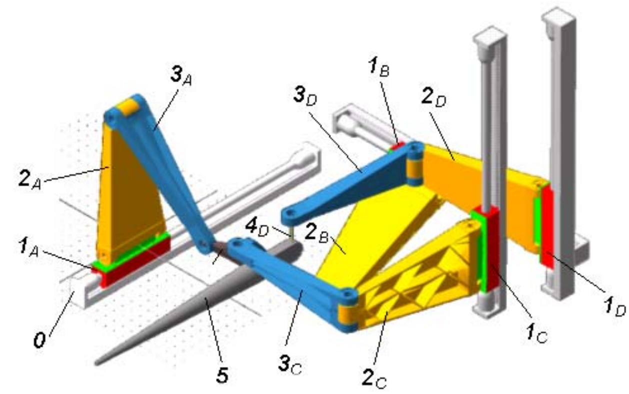

FIG 3. The CAD model of a T3R1 parallel mechanism [7]

The direct kinematic model becomes

$$\begin{bmatrix} \dot{x}_H \\ \dot{y}_H \\ \dot{z}_H \\ \dot{\varphi}_y \end{bmatrix} = \begin{bmatrix} 1 & 0 & 0 & 0 \\ 0 & 1 & 0 & 0 \\ 0 & 0 & 1 & 0 \\ 0 & 0 & 0 & b_{44} \end{bmatrix} \begin{bmatrix} \dot{d}_{10A} \\ \dot{d}_{10B} \\ \dot{d}_{10C} \\ \dot{d}_{10D} \end{bmatrix} \tag{4}$$

with

$$b_{44} = \frac{1}{r \cos \varphi_y}. \tag{5}$$

In the next sections we present the study of rigidity of a prototype of *T3R1* parallel manipulator with respect to the solution presented in Fig.1. This prototype, presented in Figs. 3 and 4, is in construction at LaRAMA - French Institute of Advanced Mechanics.

3 Preliminary design

A first preliminary CAD model (Fig. 3) was constructed based on the kinematic model of *T3R1* robot This model demonstrates feasibility of the robot and absence of collision between parts [7].

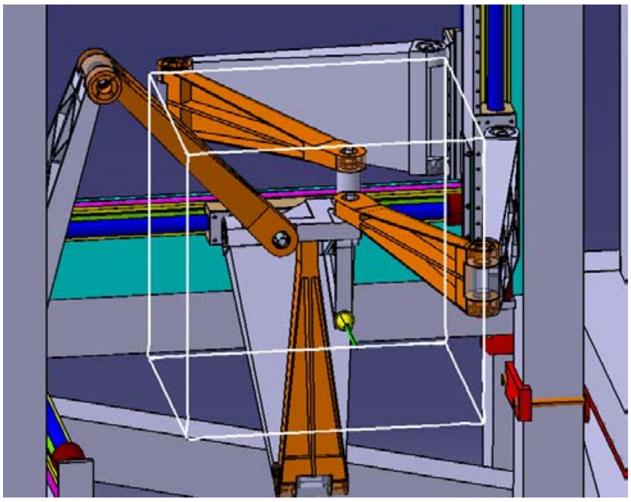

FIG 4. T3R1 robot in its rigid frame [8]

T3R1 robot is then integrated in a frame which was designed to be several orders of magnitude more rigid than the robot (Fig. 4). The white cube shown in Fig. 4 represents the maximum workspace corresponding to translation joint limits. It is now important to determine static rigidity maps of the robot in order to understand its weak points, singular configurations and later, use it for smart control.

4 Stiffness study of one leg

As *T3R1* is made of four identical legs, we will focus on the rigidity behavior of one leg (Figs. 5 and 6). It is made of two parts with a folding angle α varying from $15°$ to $165°$ in order to avoid singular configuration. We note that singular configurations occur at $\alpha = k\pi$ (k=0; 1).
Based on the CAD model of each leg, a finite element model was constructed. Each leg part is made of two tips with bearing cages connected by strengthening ribs. The bearing cages are meshed with solid elements (8 nodes with 3 DOF *x, y, z* on each). The ribs are meshed with shell elements (4 nodes with 6 DOF *x, y, z, rotx, roty, rotz* on each) in order to take bending into account. Both types of elements are connected by equalizing translation DOF and canceling rotation DOF on the boundary.
The revolute joint between parts is created by four pairs of spring elements set on cardinal points of the joint with quasi infinite stiffness (Fig. 7). In each pair, one spring is for blocking radial displacement, the other for axial displacement. The only remaining DOF is rotation around revolute axis.
The leg is considered to be fixed with a given α angle and submitted to a force F_i on one end along axis $\boldsymbol{x_i}$.
The FEM calculations gives us the Δx_i displacement of the application point of the force and equation (6) gives rigidity k_i along $\boldsymbol{x_i}$.

$$k_i = F_i / \Delta x_i \; . \qquad (6)$$

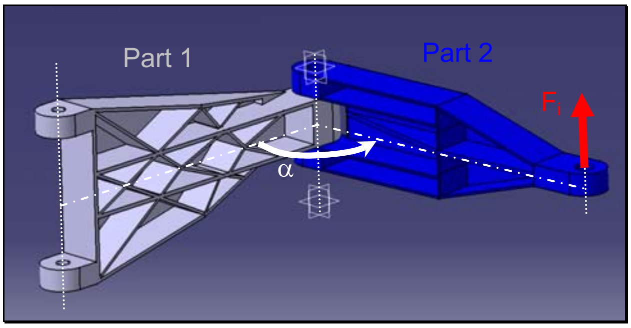

FIG 5. A refined CAD model of one leg, made of two parts with α angle and subject to force F.

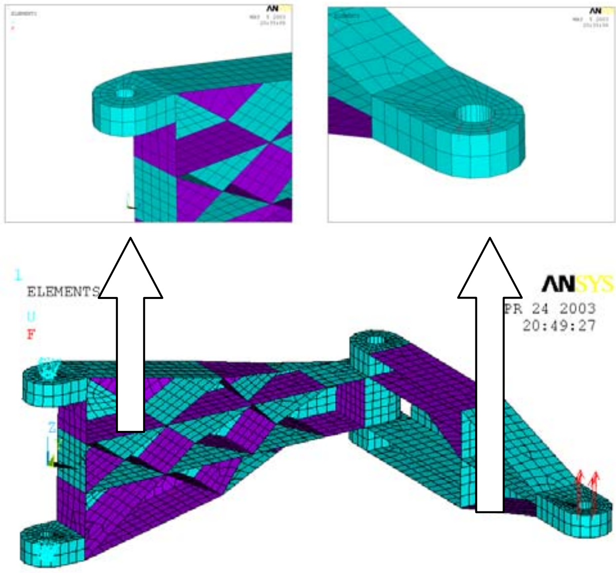

FIG 6. FEM model of one leg with details of the bearing cages on parts

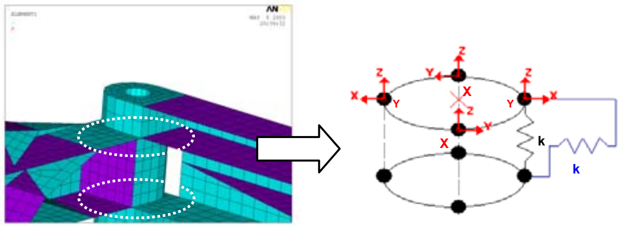

FIG 7. Revolute joint between parts is created via spring element Matrix 27 (only one couple of springs is shown for simplicity)

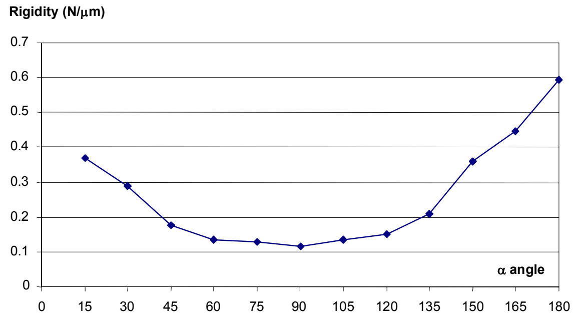

FIG 8. Rigidity results for one leg

By repeating this calculation for various values of angle α, a graph of rigidity can be drawn (Fig. 8). It appears that rigidity is far smaller for angles of 90°. This can be explained by the combination of two phenomena: torsion of part 1 of the leg superimposed on bending of the whole leg. Moreover, if we examine orders of magnitudes, it may be noticed that torsion phenomenon (maximum at 90°) is more dangerous than bending (best visible at 15° and 165°). This is an important fact that will be reproduced on each of the four legs of the robot.

5 Stiffness study of the whole robot

After meshing the four legs, adding the connecting parts and defining each revolute joint a global meshed FEM model of *T3R1* can be obtained (Fig. 9). It is fully parametrized by position and angle of end effector. Several analysis types are achieved from the finite element model. Static and modal performances reflect robot precision. Their characterization overall the work space is useful for mechanical design and control strategy optimization.

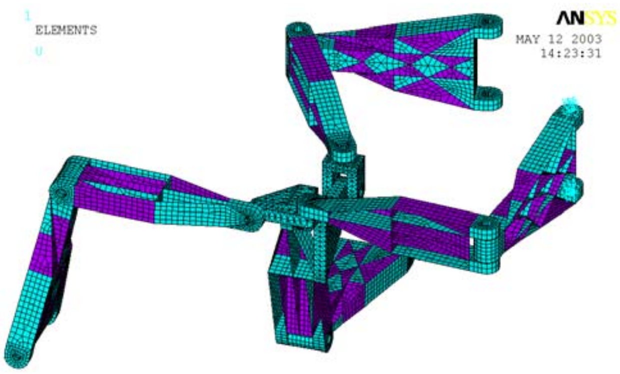

FIG 9. FEM model of the full T3R1 robot

5.1 Static rigidity characterization

Static rigidity is defined as the 6×6 symmetrical matrix $\mathbf{R}$ that maps generalized infinitesimal displacements (3 translations and 3 rotations) of the end effector to generalized external loads (3 forces and 3 torques) applied to it. Generalized displacements are defined by the vector $\mathbf{u}=[u_1 \quad u_2 \quad u_3 \quad u_4 \quad u_5 \quad u_6]^T$ where $[u_1 \quad u_2 \quad u_3]^T$ are the three translations and $[u_4 \quad u_5 \quad u_6]^T$ are the three rotations. Generalized external loads are defined by the vector $\mathbf{F}=[F_1 \quad F_2 \quad F_3 \quad F_4 \quad F_5 \quad F_6]^T$ where $[F_1 \quad F_2 \quad F_3]^T$ are the applied forces and $[F_4 \quad F_5 \quad F_6]^T$ the three applied torques at the end effector. We have

$$\mathbf{F}=\mathbf{R}\mathbf{u} \tag{7}$$

In order to identify the 21 terms of the matrix $\mathbf{R}$, 6 linearly independent load cases must be studied. By applying a force or a torque F_i, $i=1\cdots6$, we obtain, using the finite element model a generalized displacement vector $\mathbf{u}_i=[u_{i1} \quad u_{i2} \quad u_{i3} \quad u_{i4} \quad u_{i5} \quad u_{i6}]^T$. Compliance terms s_{ij}, $j=1\ldots6$ are defined by the following relation

$$s_{ij}=\frac{u_{ij}}{F_i} \tag{8}$$

Assuming that the structure is linear, superposition principle can be applied. Thereafter, for any arbitrary applied load $\mathbf{F}$, terms of resulting displacement vector are given by

$$u_j=\sum_{i=1}^{n}F_i s_{ij} \tag{9}$$

Which can be written in a matrix form

$$\mathbf{u}=\mathbf{S}\mathbf{F} \tag{10}$$

where $\mathbf{S}$ is a compliance matrix having s_{ij} as general term. Using equations (6) and (9), we obtain the rigidity matrix

$$\mathbf{R}=\mathbf{S}^{-1} \tag{11}$$

In order to characterize robot static rigidity over all the workspace, a design for experiment technique is adopted. It is based on the parametrized finite element model of the robot. The cost and the precision of such analysis depend on the number of calculation points. A full factorial, 5^3, experiment design is used with three variables and five levels. We apply 6 load cases, $F_1=F_2=F_3=3000\,\mathrm{N}$ and $F_4=F_5=F_6=24000\ \mathrm{N\cdot mm}$, for each measurement point k, $k=1\ldots125$. Compliance matrix terms, $s_{ij,k}$, are firstly determined at each point and approximated by quadratic polynomial fitting according to Cartesian coordinates of the end effector. The adopted regression functions have the following form:

$$
\begin{aligned}
s_{ij,k} &= a_{1,ij} x_k{}^2 + a_{2,ij} y_k{}^2 + a_{3,ij} z_k{}^2 \\
&+ a_{4,ij} x_k y_k + a_{5,ij} y_k z_k + a_{6,ij} z_k x_k \\
&+ a_{7,ij} x_k + a_{8,ij} y_k + a_{9,ij} z_k x_k \\
&+ a_{10,ij}
\end{aligned}
\tag{12}
$$

(x_k, y_k, z_k) are the coordinates of k^{th} measurement point. $a_{l,ij}$, $l = 1 \dots 10$, are the regression functions coefficients. They are identified in least square meaning. Let $\mathbf{x}_{ij} = [a_{1,ij}, \dots, a_{10,ij}]^T$ be the coefficients vector and $\mathbf{b}_{ij} = \left[u^1{}_{ij}, \dots\dots, u_{ij}^{125}\right]^T$ the vectors of displacements in measurement points. In optimal case, the coefficients verify the relation

$$\mathbf{A}\mathbf{x}_{ij} = \mathbf{b}_{ij} \tag{13}$$

where $\mathbf{A}$ is a 125×10 matrix given by

$$
\mathbf{A} = \begin{bmatrix}
x_1^2 & y_1^2 & \cdots\cdots & z_1 & 1 \\
\vdots & & & & \vdots \\
x_k^2 & y_k^2 & \cdots\cdots & z_k & 1 \\
\vdots & & & & \vdots \\
x_{125}^2 & y_{125}^2 & \cdots\cdots & z_{125} & 1
\end{bmatrix}
\tag{14}
$$

$\mathbf{A}$ is the same for all compliance terms and coefficients can be determined by using pseudo-inverse matrix

$$\mathbf{x}_{ij} = \left(\mathbf{A}^T \mathbf{A}\right)^{-1} \mathbf{A}^T \mathbf{b}_{ij} \tag{15}$$

Rigidity matrices at each point are obtained by the inversion of compliance matrices. The evolution of the robot rigidity can be represented by 3D maps for a constant values of the *y* coordinate. In Fig. 10, terms of translation rigidity are fitted for *y* =250 mm. The highest rigidity term is R_{zz} along the *Z* direction. This can be explained by the use of two legs in this direction. Rigidities along *X* and *Y* directions, R_{xx} and R_{yy}, are of same order. We notice the strong rigidity coupling, R_{yz}, between *Z* and *Y* directions. On the other hand *X* and *Y* rigidities are weakly coupled especially for small values of *x*. The global rigidity of robot along a direction is greater then the rigidity of an isolated leg due to rigidity couplings.

5.2 *Modal characterization*

A modal analysis of the robot is performed. Natural frequencies reflect the robot dynamic rigidity and precision. In order to characterize robot natural frequencies over all the workspace, we adopt the same technique used for static rigidity characterization. The three first modes are considered.

The evolution of natural frequencies over the workspace is presented by 3D maps for a constant *y* coordinate. Surfaces have sensibly the same shape for the 3 modes (Fig. 11). The minimum natural frequency is about 40 Hz.

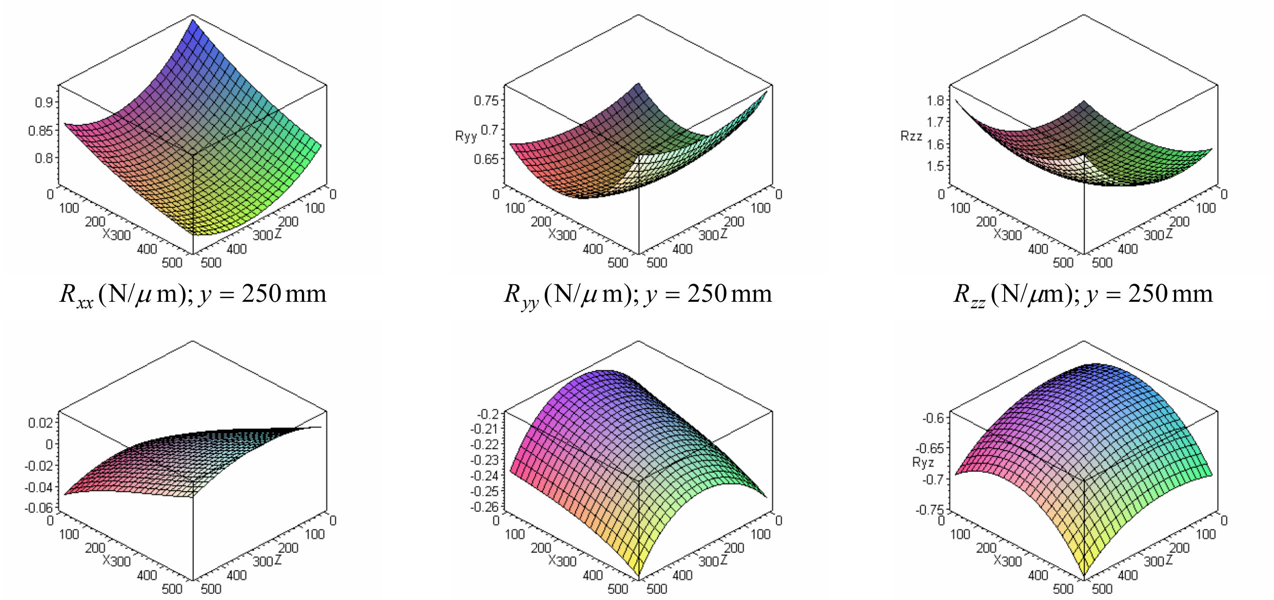

R_{xx} (N/μm); $y = 250$ mm

R_{yy} (N/μm); $y = 250$ mm

R_{zz} (N/μm); $y = 250$ mm

R_{xy} (N/μm); $y = 250$ mm

R_{xz} (N/μm); $y = 250$ mm

R_{yz} (N/μm); $y = 250$ mm

FIG. 10. Static rigidity maps

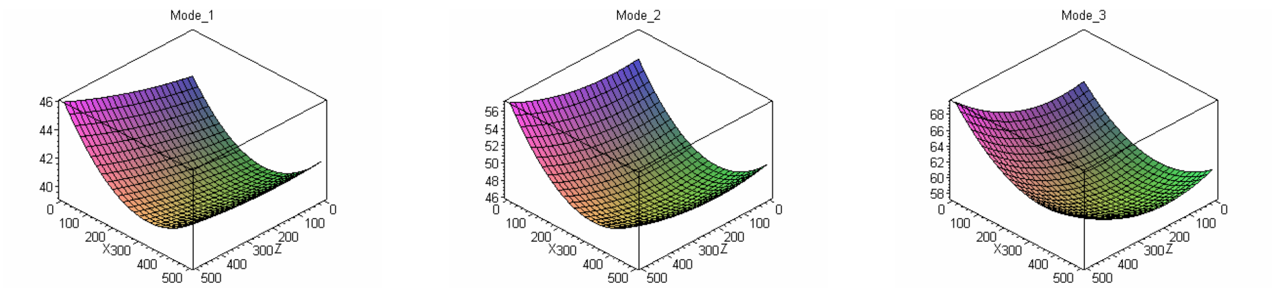

FIG 11. Natural frequencies maps (Hz) $y = 250\,\text{mm}$

6 Conclusion

The paper presents static rigidity and natural frequencies of *T3R1*, a new parallel platform mechanism with four degrees of mobility and pseudo-decoupled motions developed at LaRAMA - French Institute of Advanced Mechanics. *T3R1* is composed of a mobile platform and a base connected in parallel by four legs. Under the action of the total constraints of its four legs, the mobile platform can do three independent translations (x_H, y_H, z_H) and one rotation φ_a (a=x,y,z). The solution analyzed in this paper allows a rotation on y axis (a=y). Each leg has three revolute joint axes parallel to the ground-connected prismatic joint axis and the mobile platform is connected by two revolute joints parallel to a axis (a=y). The four ground-connected prismatic joints are actuated. Rigidity study is achieved by using FEM. The influence of the folding angle on the rigidity of each leg has shown that rigidity is far smaller for angles of about 90°. This can be explained by the combination of two phenomena: torsion of part 1 of the leg superimposed on bending of the whole leg. Moreover, if we examine orders of magnitudes, it may be noticed that torsion phenomenon (maximum at 90°) is more dangerous than bending (maximum at 15° and 165°). Based on the parametrized FEM model, a design for experiment technique was adopted in order to characterize robot static rigidity and natural frequencies over all the workspace. A full factorial, 3^5, experiment design was used with three variables and five levels. Rigidity study of the whole robot have indicated a strong rigidity coupling, R_{yz}, between Z and Y directions. On the other hand X and Z rigidities are weakly coupled. The global rigidity of robot along a direction is greater then the rigidity of an isolated leg. This is due to rigidity couplings. The modal analysis of the robot first three modes have indicated a minimum natural frequency of about 40 Hz. These preliminary results allow us to conclude that parallel robots with decoupled motions such as T3R1 have a wide range of potential applications in manipulation, assembling and machining.

Acknowledgment

This study was jointly funded by the MAX project within the CNRS-ROBEA 2001-2003 program and by CPER Auvergne 2002-2004 program.

References

[1] G. Gogu, Structural synthesis of parallel robotic manipulators with decoupled motions. Internal Report ROBEA MAX - CNRS, 2002.

[2] J.M. Hervé, F. Sparacino, Structural synthesis of "parallel" robots generating spatial translation. Proceedings of the 5th International Conference on Advanced Robotics, Pisa, Italy, vol. 1, 808-813.

[3] M. Carricato, V. Parenti-Castelli, Singularity-free fully-isotropic translational parallel mechanism, International Journal of Robotics Research 21(2) (2002) 161-174.

[4] H. S. Kim, L-W. Tsai, Evaluation of a Cartesian parallel manipulator, Advances in Robot Kinematics, edited by J. Lenarcic and F. Thomas, Kluwer Academic Publishers, 2002, pp.21-28.

[5] X. Kong, C. M. Gosselin, Type synthesis of linear translational parallel manipulators, Advances in Robot Kinematics, edited by J. Lenarcic and F. Thomas, Kluwer Academic Publishers, 2002, pp.453-462.

[6] J-P. Merlet, Les Robots Parallèles, Hermes, Paris, 1997.

[7] F. Morellec, Conception du robot parallèle *T3R1*, Projet CNAM, 2003, LaRAMA-IFMA.

[8] L. Lecerf, Conception du bâti du robot parallèle T3R1, Projet de Fin d'Etudes 2003 , LaRAMA-IFMA.

[9] Y. Heerah, Etude de la rigidité statique et dynamiquedu robot parallèle T3R1, Master Thesis, LaRAMA-IFMA and University of Bath.